



Investigation on the Effect of Different Pre-Cracking Methods on Fracture Toughness of RT-PMMA

Abstract

In this study, eight techniques including coping saw, metal slitting saw, razor blade, cubic boron nitride (CBN) disc, scoring, die-cutting and guillotining, diamond disc, and laser cutting methods were used to produce pre-cracked fracture toughness (K_{Ic}) test specimens made of poly(methyl methacrylate)/graft-acrylonitrile butadiene styrene blends. The influences of notch shape (radial, rectangular, or angular-shaped and variety of thicknesses), pre-cracking method, chip removing or non-chip removing, and the contact or non-contact methods on the results obtained in fracture toughness tests were investigated. The results were analyzed by two methods, quantitatively and qualitatively, by comparing the obtained K_{Ic} results and studying the SEM and optical microscopy images, respectively. The results indicated that the different conditions of a produced pre-crack including; geometry of pre-crack due to geometry of tools, residual stress due to pre-crack creation, heat affected zone, damage of crack tip, and producing crazing around the crack tip could affect the fracture toughness. The maximum difference resulted from different pre-cracking methods was equal to $0.24 \text{ MPa}\cdot\text{m}^{0.5}$ and the lowest value of fracture toughness K_{Ic} , $2.53 \text{ MPa}\cdot\text{m}^{0.5}$, belonged to the scoring method but the highest value, $2.77 \text{ MPa}\cdot\text{m}^{0.5}$, belonged to the metal slitting saw method. Also, the results indicated that the effects of notching on toughness of RT-PMMA had a low notch sensitivity and the differences between minimum and maximum K_{Ic} values was found about 9%.

Keywords

Pre-cracking methods, Rubber-toughened PMMA, Fracture toughness, Crack tip shape, Critical stress intensity factor.

Elyas Haddadi^a

Naghdali Choupani^b

Farhang Abbasi^c

^a PhD Student, Faculty of Mechanical Engineering, Sahand University of Technology, Tabriz, Iran, e_haddadi@sut.ac.ir

^b Associate Professor, Faculty of Mechanical Engineering, Sahand University of Technology, Tabriz, Iran, choupani@sut.ac.ir

^c Professor, Institute of Polymeric Materials, Sahand University of Technology, Tabriz, Iran, f.abbasi@sut.ac.ir

<http://dx.doi.org/10.1590/1679-78252804>

Received 20.01.2016

In revised form 23.05.2016

Accepted 24.05.2016

Available online 07.06.2016

1 INTRODUCTION

The utilization of polymers is getting more and more due to their wide range of applications in various fields. In the meantime, the usages of materials like steels, silica, glasses, etc. are slowly

being substituted by polymers. In this regard, applications of thermoplastic poly(methyl methacrylate) (PMMA) and PMMA containing compounds have grown considerably in many cases, for example, airplane, automobile, building industry, lenses, light pipes, and toys due to its light weight and suitable mechanical and physical properties (Souza J. et al. 2012). Because of the brittleness of thermoplastic PMMA, toughening them with different methods or incorporating other materials like graft-acrylonitrile-butadiene-styrene (g-ABS) blends broadens its usages.

To recognize the position of a new compound of a polymer material like PMMA, studying and enhancing the fracture toughness is required. To study the fracture mechanics of different materials, first of all, pre-cracking of the specimens is required to simplify the study of the results for making them acceptable, therefore creating standard pre-cracks are essential to obtain an acceptable mechanical result. Pre-cracking in polymers is crucial (Salazar A. & Patel Y. 2013). Since creating a pre-crack according to ASTM and ESIS standards, even from fatigue method, due to hysteretic heating, is not possible (Salazar A. & Patel Y. 2013). Therefore, several methods have been declared in many papers to create a natural crack in different polymeric materials (Salazar A. & Patel Y. 2013, Cayard M. & Bradley W. 2013, Peres F.M. et al. 2010, Peres F.M. et al. 2014, Oskui, A.E. et al. 2016, Yan J. et al. 2008, Wei Y. et al. 1990, Hashemi S. & Williams J. 1984). According to the standards, the crack tip radius must be lower than 20 μm (Salazar A. & Patel Y. 2013). Approximately, none of these methods may not produce the similar samples (Kruzic J. et al. 2005). The type of pre-crack creating process depends on the material consisting of the sample. While a pre-crack has been produced by tapping, sliding, pressing, and sawing a razor blade for many materials, tapping razor blade method has been utilized to produce a pre-crack in PMMA samples (Souza J. et al. 2012). This study, unlike previous investigations, focused one valuation of the chip and non-chip removal methods and comparing the obtained results from different methods. The reason behind the concentration on the chip removal methods was their high accuracy and monotony. Despite disadvantages like being costly and time consuming, the chip removal method has advantages like high accuracy and smooth to create a pre-crack. This method increases sample testability and avoids sample failure that causes obstacle in results due to unexpected fracture tests outcomes. The specimen's length, width and thickness, and whether the specimen is unnotched or notched and, if notched, the depth and sharpness of the notch, may all influence the observed fracture toughness (Kinloch A.J. & Young R.J. 1985, Needleman A. et al. 2005, Marshall G.P. et al. 1973, Low I.M. & Mai Y.W. 1989, Mandell J.F. et al. 1982).

In this work, chip removal (coping saw, metal slitting saw, cubic boron nitride (CBN) disk, scoring, diamond disk, and laser cutting) and non-chip removal (razor blade tapping and die-cutting or guillotine) methods were used to produce pre-crack and the fracture toughness K_{Ic} values obtained from fracture of PMMA/g-ABS specimens were compared. For this purpose, handy or machining and contact or non-contact chip removal methods were used. In the handy methods, two tools including coping saw and scoring were employed that had lower accuracy and the lowest heat affected zone and damage on crack tip region. The CNC milling machine with metal slitting saw, CBN, and diamond disk tools were used in machining methods that had higher accuracy compared with handy methods. The heat affected zones created by these methods were also considerable except the zone created by diamond disk method. The stress that may be developed inside the machined areas can cause problems during subsequent steps such as bonding. This internal stress just like that devel-

oped in molded parts has to be released by annealing. Laser cutting is one of the important non-contact methods that has the highest accuracy, repeatability and same production of specimen in among other methods (Salazar A. & Patel Y. 2013, Choudhury I. & Shirley S. 2010, Davim J.P. et al. 2008, Ghavidel A.K. et al. 2015); the heat affected zone in this method is somewhat similar with two previous methods.

Among the non-chip removal methods, die-cutting or guillotine and razor blade are widely employed. In order to prevent the pre-crack from possible deformation, damage, and crazing by guillotine method, the samples were heated at 100-140 °C before the pre-crack was produced. A tool with 0.11 mm thickness was also used in razor blade method and the specimens were produced by tapping procedure. The fracture toughness K_c values obtained from fracture of PMMA/g-ABS specimens pre-cracked with different methods were compared.

The fracture toughness represents a material intrinsic parameter, it is actually known as the value of the produced critical stress intensity factor K_c due to stress concentration at the crack tip zone when the crack is subjected to tensile stresses normal to the crack axis and the crack is called in that case mode-I crack (El-Sheikhy R. & Al-Shamrani M. 2015). The value of the fracture toughness K_c for a material was measured by testing the cracked specimens. The critical stress intensity factor at the crack tip is given by (Oskui A.E., et al. 2014):

$$K_c = \frac{P_c}{tw} \sqrt{\pi a} f\left(\frac{a}{w}\right) \quad (1)$$

where P_c is the fracture load, a represents the crack length, w stands for specimen width, t is the specimen thickness, and $f(a/w)$ is the dimensionless stress intensity factor (Gdoutos E.E. 2005).

The main objective of this study was to assess the influence of eight different pre-cracking techniques in linear elastic K_c results of RT-PMMA. Also, the results were analyzed by two methods, quantitatively and qualitatively, by comparing the obtained K_c results and studying the SEM and optical microscopy images.

2 EXPERIMENTAL DETAILS

2.1 Materials

PMMA (EG920) pellets with MFI=1.7 g/10 min, tensile strength at break $\sigma_b=74$ MPa was purchased from LG, Korea. G-ABS powder with $\bar{M}_w=300,000$ g/mol, average particle size = 0.43 μm , degree of grafting = 70-75%, rubber content = 58.5%, and glass transition temperature $T_g=90$ °C was purchased from Tabriz Petrochemical Company, Iran. The compound ratio of PMMA to g-ABS was 85/15 (wt/wt). The yield strength (σ_y) of PMMA/g-ABS compound was 44 MPa and the elastic modulus was 1.65 GPa.

2.2 Test specimens

Bath melt compounding of PMMA/g-ABS blends was carried out in a laboratory batch internal mixer (Brabender W50 EHT, Duisburg, Germany) with a 55-mL mixing chamber at 220 °C and 60 rpm for 9 min. The samples for the K_c tests were prepared by a compression molding machine (Brabender Polystat 200 T, Germany) at 230 °C and 50 bars and were cooled to ambient tempera-

ture by circulating water with a 17 ± 5 °C/min average cooling rate. The dimensions of the K_{Ic} test samples were $70 \times 25 \times 0.8$ mm³. At least seven specimens were tested for 15 mm ligament length. Eight methods were used to produce double edge notched specimens in tension (DENT) artificial crack tips (Table 1). Ligament length and specimens thicknesses were measured within ± 1 μ m.

Methods	Tools Type	Dimensions (mm)	Machining Parameters	Crack Radius (μ m)	HAZ (μ m)	Crack Width (μ m)	Damaged Zone (μ m)
Coping saw		Max. thickness: 0.3	-	-	-	220	45-90
Metal slitting saw		$\phi 40 \times 0.3$	Spindle speed: 350 rpm Feed rate: 12 mm/min	-	50	290	-
Razor blade		Max. thickness: 0.11	-	-	-	24	150
CBN disc		$\phi 60 \times 0.5$	Spindle speed: 200 rpm Feed rate: 12 mm/min	R300	40	-	-
Scoring		Max. thickness: 0.6	-	R110	-	-	-
Die-cutting and guillotining		Max. thickness: 0.6	-	-	-	160	Crazing
Diamond disc		$\phi 22 \times 0.2$	Spindle Speed: 400 rpm Feed rate: 12 mm/min	-	-	160	-
Laser cutting		-	Power: 50 W Feedrate: 20 mm/sec	R65	40	-	-

Table 1: Methods used to produce double edge notched specimens for tension tests.

2.3 Testing

All tests were carried out using a Zwick/z10 (Germany) testing machine at room temperature and crosshead speed of 1 mm/min. The loads and the crosshead displacements applied to the specimens were recorded during the experiments.

Prior to testing, the surface of each specimen was analyzed via optical microscopy (Olympus PMG3, Tokyo, Japan) and scanning electron microscopy (SEM, Tescan MIRA3, Czech Republic) to observe the crack tip front and measure the crack tip shape and evaluating fracture surface characteristics of some typical specimens. Prior to SEM investigation, the fracture surfaces were coated with a thin layer of gold.

3 RESULTS AND DISCUSSION

Figs. 1-4 show the scanning electron microscopy and optical microscopy micrographs taken from the notch zones of samples pre-cracked with different procedures. The notch inserted by metal slitting saw had a rectangular shaped (with a width of $\sim 300 \mu\text{m}$) crack tip with a heat affected zone formed around the pre-crack (Fig. 1(a)). This flat crack tip region was a case having the greatest K_{Ic} value among the other pre-cracking methods (Fig. 5). In the case of the sample notched with a diamond disc, the presence of some curvature at the tip of pre-crack and lower width of the pre-crack led to a decrease in K_{Ic} value as compared with the value measured for the sample pre-cracked with metal slitting saw method (Fig. 1(b)). No obvious deformation could be seen in the sample containing diamond disk produced notch. Although the notch inserted by the coping saw had a rectangular-shaped crack tip, but, due to the presence of a significant deformation around the notch, especially at the crack tip region, its K_{Ic} value was lower than those obtained by metal slitting saw and diamond disk pre-cracking methods (Fig. 2(a)). It is believed that the weakened material in the deformed region in front of crack tip facilitates the crack propagation through the material. The lower K_{Ic} value of the sample with pre-crack inserted by the razor blade method as compared with the sample pre-cracked by metal slitting saw, diamond disk, and coping saw could be due to the sharpness of the razor blade. However, in spite of the lowest crack width associated with the razor blade method, this method indicated a higher K_{Ic} value compared with the other methods. This might be caused by deformation of razor blade during the tapping process of notch formation, which could result in the deformation of the material near the crack tip (Fig. 2(b)).

Regarding the notch formed by the die-cutting and guillotine, the notch again had a rectangular shape at the tip. However, in spite of heating these samples at 100-140 °C, there were numerous micro-cracks craze-like features at the notch root (Fig. 3(a)). These micro-cracks were nucleated at the notch root and were propagated through the ligament of the material in front of notch. The formation and development of the deformation band in front of notch root during the high speed notch insertion by guillotine facilitated the propagation of the initial-notch through the material, which, in turn, further reduced the K_{Ic} values of the material. Development of heat affected zone in this sample, as can be seen in the optical micrograph (Fig. 3(b)), might be responsible for decreasing the K_{Ic} value of the sample pre-cracked by CBN disk. On the other hand, the notch inserted by the laser cutting method had the lowest crack tip radius among the notches with circular-shaped tips (Fig. 4(a)). This geometrical difference along with the formation of a heat affected zone around

the pre-crack, applied by laser pre-cracking method, greatly decreased the crack resistance of the sample with laser notch. Among the different pre-cracking methods studied in this work, the sample notched by scoring method showed the lowest value of K_{Ic} parameter (Fig. 5). According to SEM and optical micrographs of this sample (Fig. 4(b)), the notch inserted by scoring had a cone-shape with a relatively sharp crack tip. Therefore the intensity of the stress field and triaxiality of the stress state was very high at the crack tip region, which significantly reduced the K_{Ic} value of the material.

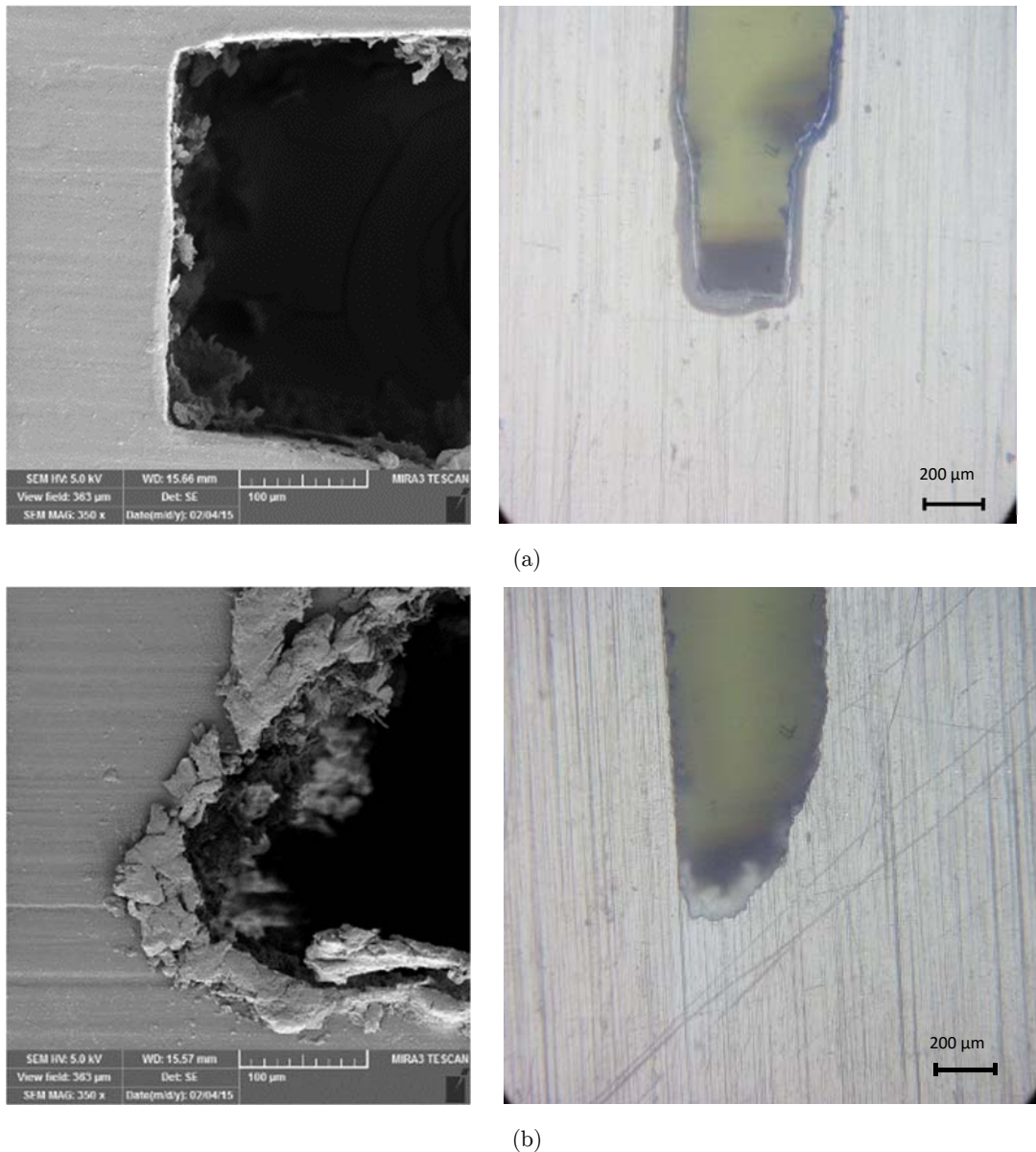


Figure 1: SEM (left images) and optical (right images) micrographs of notch roots produced by (a) metal slitting saw and (b) diamond disk.

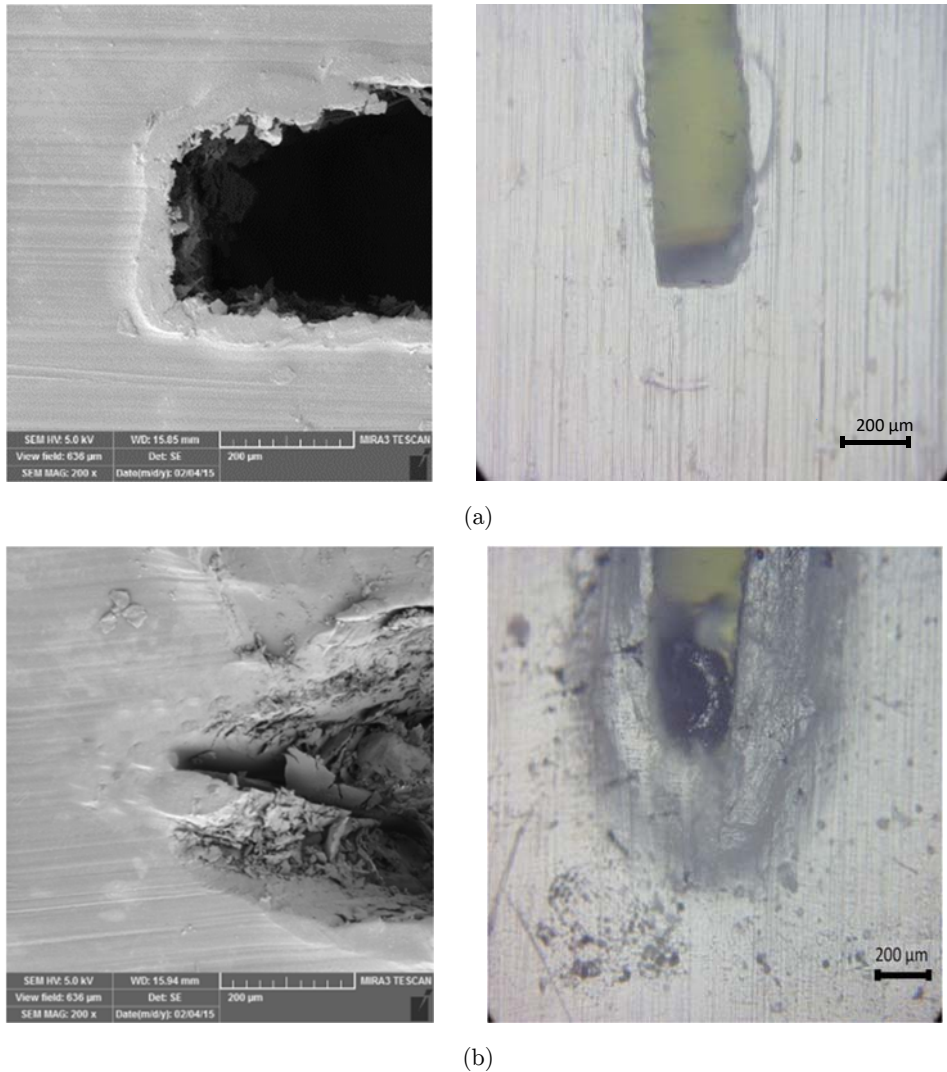


Figure 2: SEM (left images) and optical (right images) micrographs of notch roots produced by (a) coping saw and (b) razor blade.

Fig. 6 shows typical load-displacement curves of the eight different samples pre-cracked by different procedures. The load-displacement behavior of the samples pre-cracked with razor blade, CBN disk, and diamond disk method was almost the same up to about 0.48 kN. The behavior of other samples was similar up to about 0.41 kN. The maximum load values, however, were different for various methods. The parameters and the calculated critical stress intensity factor, K_{Ic} , values were listed in Table 2 and shown graphically in Fig. 5. As expected, the fracture toughness changed with the notch tip radius, rectangular shape, and the damaged crack tip. The value of the fracture toughness was also affected by heat affected zone. The highest value of fracture toughness values was $2.77 \text{ MPa}\cdot\text{m}^{0.5}$ belonging to metal slitting saw method with the largest crack tip of rectangular shape ($= 290 \text{ }\mu\text{m}$) (Table 1). Scoring method had the lowest fracture toughness values, 2.53

MPa.m^{0.5}, with a crack tip radius, R110 μm (Table 1), and no sign of deformation and heat affected zone at the crack tip (Fig. 4(b)).

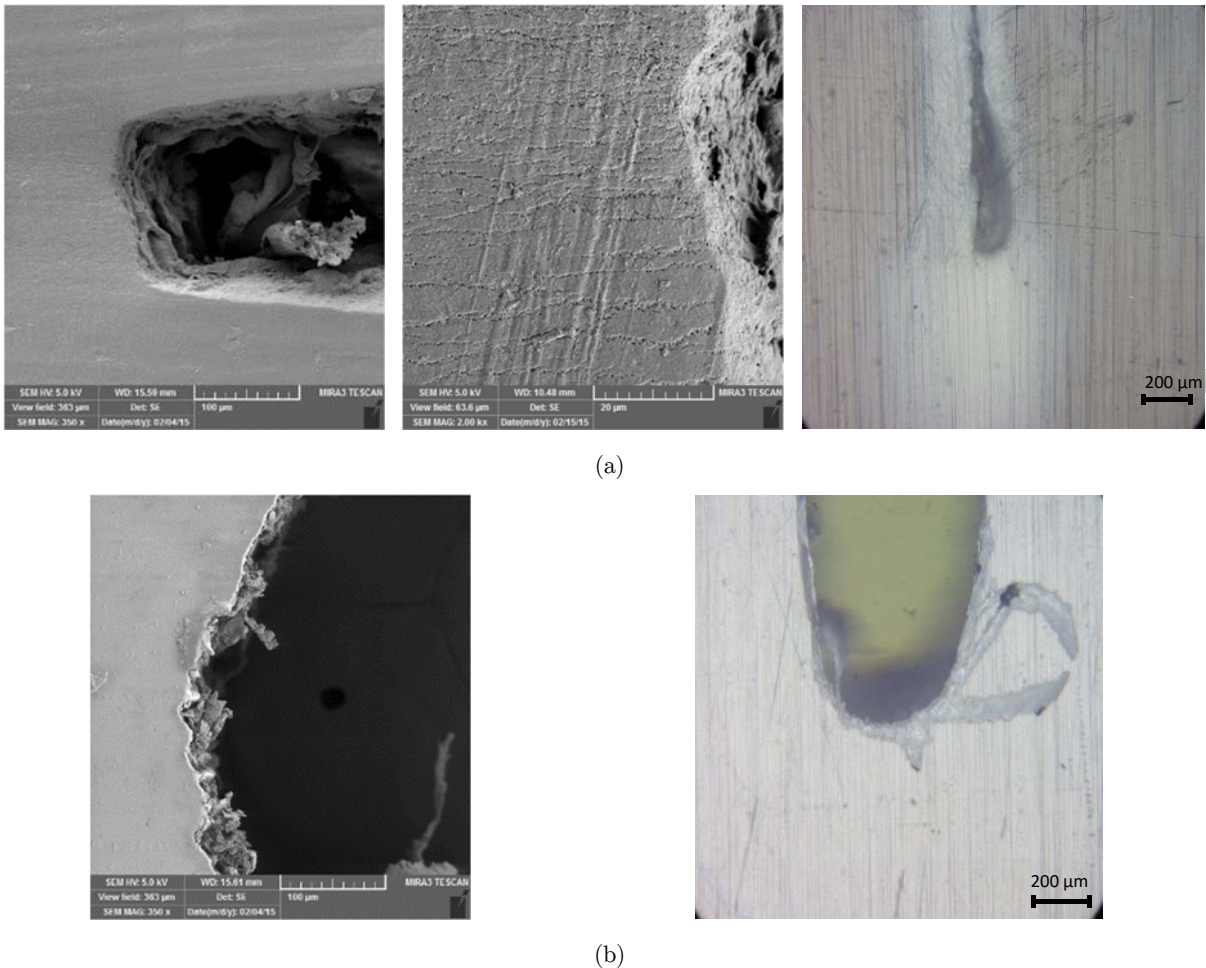


Figure 3: SEM (left images) and optical (right images) micrographs of notch roots produced by (a) die-cutting and guillotine, with different magnification and numerous micro-cracks craze-like features at the notch root (middle image) and (b) CBN disk.

ASTM standard test methods for fracture mechanics testing of polymers, ASTM D5045 for plane strain fracture toughness test and ASTM D6068 for J-R curve determination give some guidance about the use of notched samples containing a pre-crack and allow inserting the pre-crack by sliding the razor blade. ASTM standard fracture toughness tests require the use of a natural crack for polymers by tapping on a fresh razor blade placed in the root of a previously machined notch, and warn against producing the pre-crack by pressing the razor blade, since this could lead to residual stresses at the crack tip, which could affect the measured fracture toughness values (ASTM D6068 also allows fatigue pre-cracking provided hysteretic heating can be avoided).

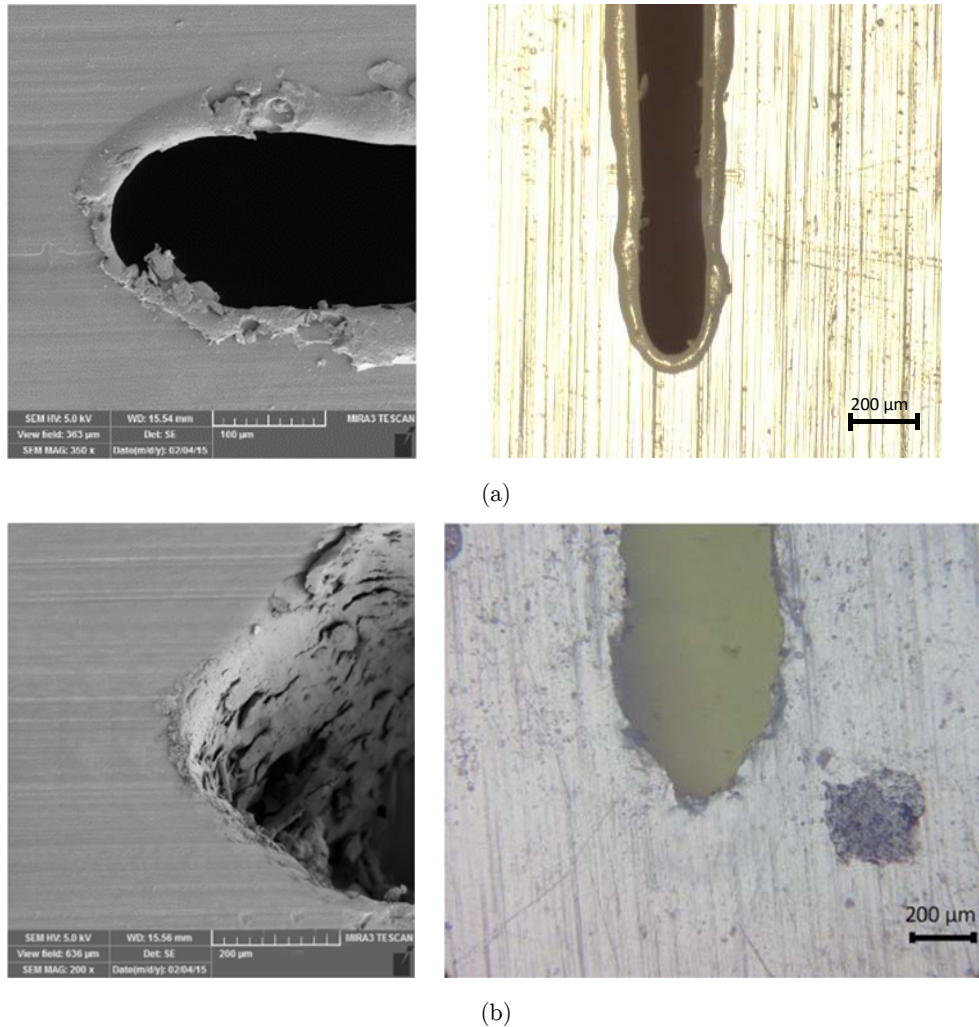


Figure 4: SEM (left images) and optical (right images) micrographs of notch roots produced by (a) laser cutting and (b) scoring.

The fracture behavior of poly(methyl methacrylate)/graft-acrylonitrile butadiene styrene blends has been evaluated using eight techniques including coping saw, metal slitting saw, razor blade, cubic boron nitride (CBN) disc, scoring, die-cutting and guillotining, diamond disc, and laser cutting methods. The resulting values of the fracture toughness are shown in Fig. 5 and are summarized in Table 2. The fracture toughness of RT-PMMA was less sensitive to the pre-cracking methods. The scoring and laser cutting methods produces small pre-crack tip radius, hardly causes residual stress around the pre-crack tip and gives lower values of fracture toughness. The metal slitting saw, diamond disc and coping saw methods can induce a large amount of plastic deformation and induced compressive residual stress around the pre-crack tip and is the essential factor responsible for high value of fracture toughness. The specimens pre-cracked by the remaining methods all contained regions of stress-free material ahead of the crack tip and hardly causes residual stress around the pre-crack tip which gave lower values of fracture toughness. The results of this work showed

that only utilization of sharp and thin tools could not be a reason to produce a sharp pre-crack. Since the tools might be deformed during producing pre-cracks, which causes damage in front of crack tip. This phenomenon, which alters the fracture toughness of samples, was observed in the case of razor blade. The obtained fracture toughness values showed that in addition to the geometry of crack tip, the fracture toughness strongly depended on crack tip radius, crack width, and angular or rectangular shape. Moreover, the damage in front of crack, heat affected zone, and residual stress could be effective on the fracture toughness of samples. Therefore, to decrease the mentioned effects on the fracture toughness of polymeric materials, it would be better to select the method of pre-crack production based on the material type.

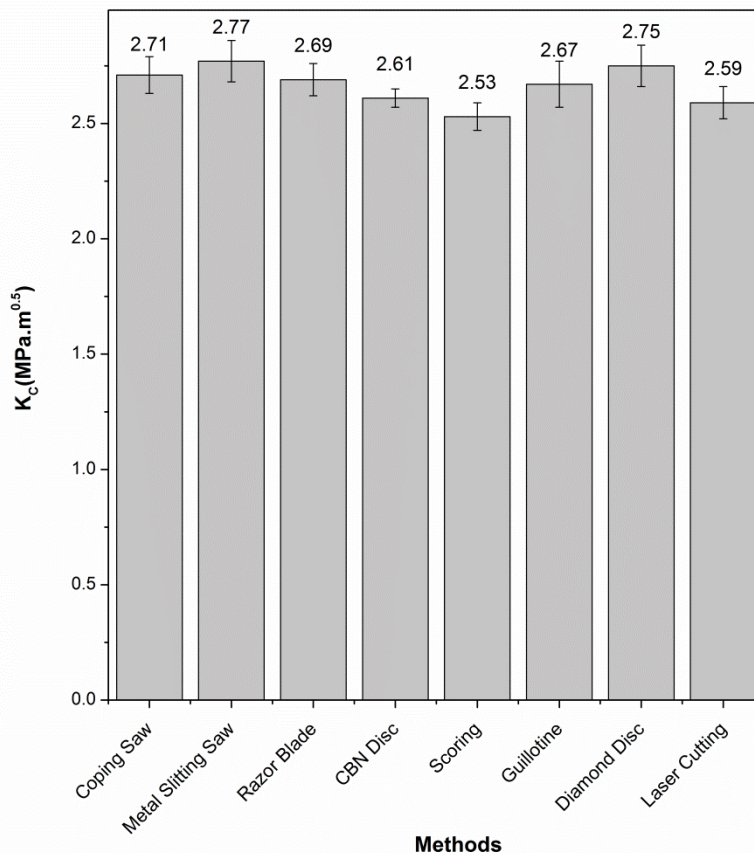


Figure 5: The critical stress intensity factor, K_c , values as a function of notching procedure.

Table 2 shows the results of the eight sets of samples investigated in the present work. As it can be seen from the table, a simple statistical analysis can be applied to compare the average fracture toughness values. By comparing the results, it can be concluded that with about 90% significance level, the fracture toughness values are affected by the pre-cracking method and the effects of notching on toughness of RT-PMMA had a low notch sensitivity and the differences between minimum and maximum fracture toughness values was found about 9%. This difference in fracture toughness values seems to be the state of the polymer during pre-cracking and not during testing.

Further research using various polymers are needed in order to obtain a pattern, but it is clear that various polymers require different pre-cracking methods and there is no standard pre-cracking technique valid for every polymer, as in the case for metals and alloys (fatigue pre-cracking method).

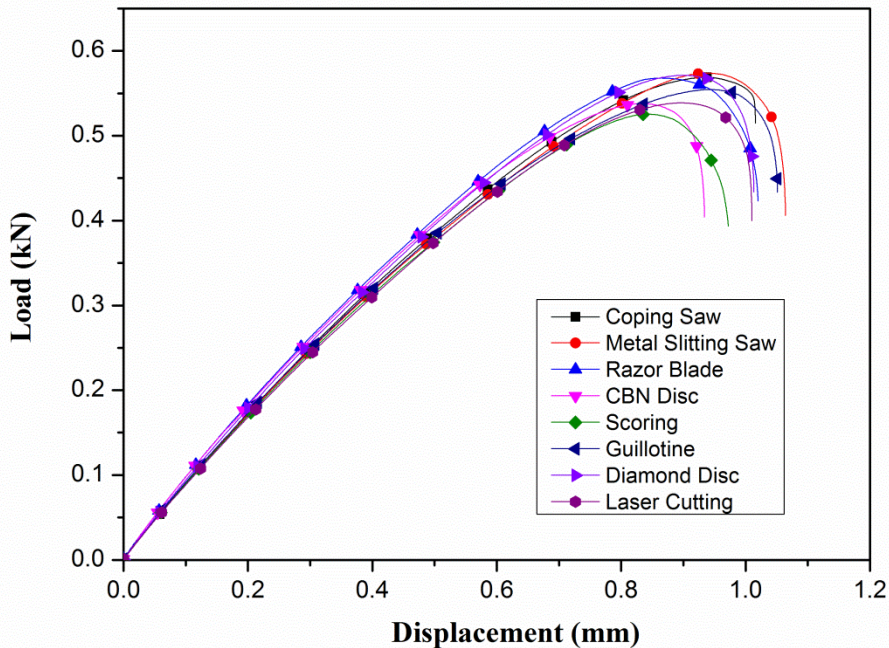


Figure 6: Load-displacement curves of PMMA/g-ABS (85/15) blends at double end crack length 5 mm (ligament length 15 mm) pre-cracked with different methods.

Pre-cracking method	w (mm)	t (mm)	a (mm)	P_{\max} (N)	K_{Ic} (MPa.m ^{0.5})
Copping saw	25	0.8	5	563	2.71±0.08
Metal slitting saw	25	0.8	5	574	2.77 ±0.09
Tapping a razor blade	25	0.8	5	559	2.69 ±0.07
CBN disc	25	0.8	5	538	2.61 ±0.04
Scoring	25	0.8	5	525	2.53 ±0.06
Die-cutting and guillotining	25	0.8	5	554	2.67 ±0.1
Diamond disc	25	0.8	5	571	2.75 ±0.09
Laser cutting	25	0.8	5	538	2.59 ±0.07
Mean ±SD					2.67±0.08

Table 2: The values of K_{Ic} for the samples pre-cracked by different methods.

3.1 Fractography

Figs. 7-9 show some typical examples of the SEM micrographs taken from the middle portion of the fracture surface with different magnifications. These micrographs belonged to the produced surface at the last step of the fracture process of PMMA/g-ABS compounds containing 15 wt% rubber

phase. The structure of the fracture surface and the stress whitening zone indicated in the micrographs give information about the deformation mechanism happening in a double end notch tensile specimen and the stability of the propagating crack. The ligament yielded before crack growth in a notched specimen under a low strain. In crack growth, the already yielded material continued to deform, mainly at the crack tip, until the fracture. In the case of metal slitting saw method, an extensive microvoid formation was apparent on the fracture surface, along with the drawing of the material in the direction of the applied tensile stress. Because of the strong adhesion between the dispersed rubber particles and matrix, through attractive interaction between styrene-acrylonitrile copolymer (SAN) chains grafted to the particles and the PMMA matrix, the void formation could be attributed to the rubber particle cavitation. However, debonding at the interface between the rubber particles and the matrix at the final stages of fracture might have partly contribution to the void formation (Mazidi M.M. et al. 2014). These processes played an important role in determining the toughness of the rubber-modified polymers. The cavitation process is usually accompanied by other processes. The combination of the plastic deformation of the fracture surface the ductile deformation of the matrix materials ahead of the crack was shown to be enhanced by cavitation. Therefore, it was reasonable to conclude that in this composition, the plastic damage mechanism was the shear yielding of the matrix, which was promoted by cavitation. The mechanism of the shear yielding of the matrix enhanced by the cavitation was explained by the different moduli of the matrix and rubber particles. Once uniaxial tensile stress was applied to the specimen, the stress concentrated around the modifier particles, and the maximum stress concentration occurred at the equator of the modifier particle (Mazidi M.M. et al. 2014). This stress concentration gave rise to a higher hydrostatic stress inside the particle. This triaxial stress caused the slight volume dilatation in the rubber particles. When the triaxial stress reached its maximum, one microvoid appeared in the plastically stretched rubber particle and caused the partial release of triaxial stress. As soon as a particle cavitated, shear yielding propagated in the matrix around this particle until it reached another particle, which cavitated in turn. The number of cavitated particles increased steadily with strain. The prerequisite for this cavitation was strong interfacial adhesion between the rubber particles and the matrix.

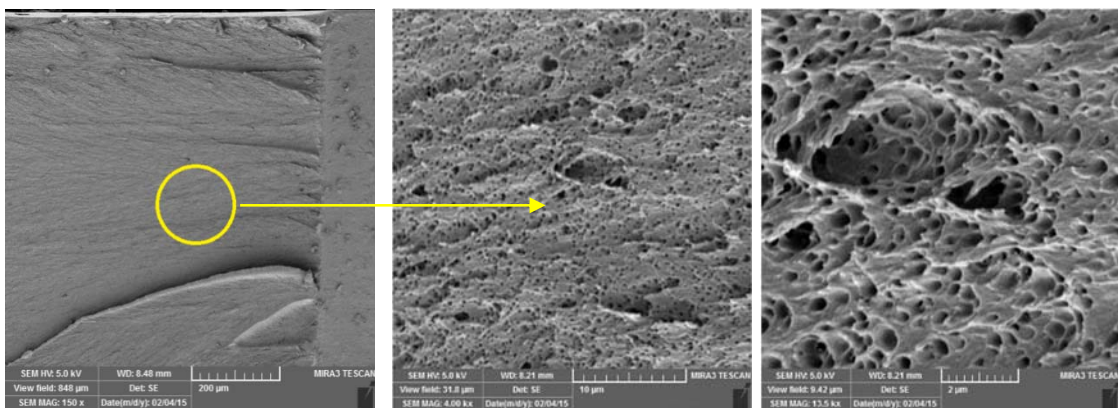


Figure 7: SEM micrographs of fracture surface of a specimen with a rectangular crack tip with different magnifications (specimen produced using a metal slitting saw, crack width = 290 μm).

Metal slitting saw method had the highest critical stress intensity factor.

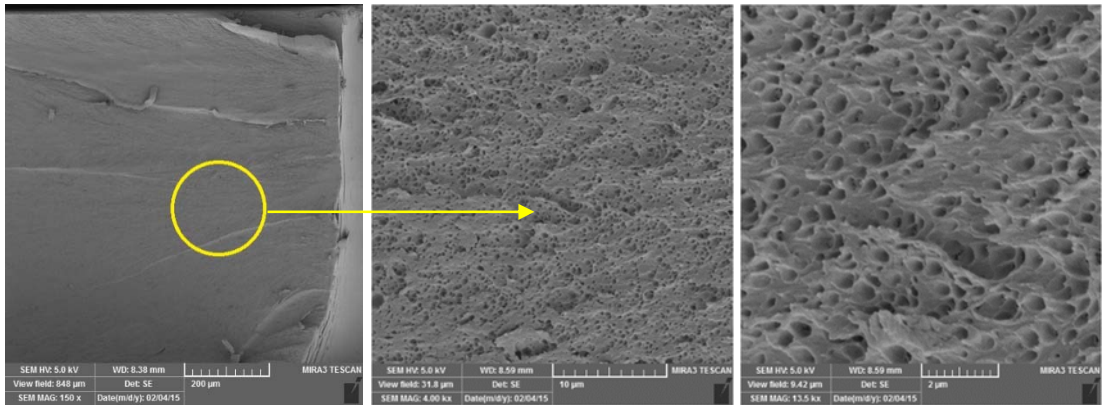


Figure 8: SEM micrographs of fracture surface of a specimen with a sharp crack with different magnifications (specimen sharpened using a laser cutting, crack radius = $R65 \mu\text{m}$). Laser cutting method exhibited the critical stress intensity factor lower than that for metal slitting saw method and greater than scoring method.

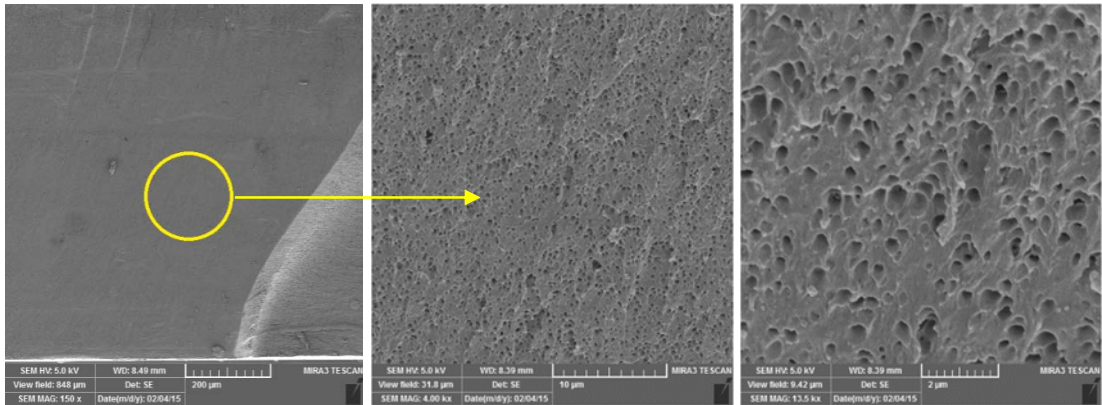


Figure 9: SEM micrographs of fracture surface of a specimen with a sharp crack with different magnifications (specimen sharpened using a scoring, crack radius = $R110 \mu\text{m}$). Scoring method had the lowest critical stress intensity factor.

In the case of metal slitting method (Fig. 7), the number of microvoids, the extent of stress whitening, and the size of microvoids were higher than those for two other methods. This different behavior was also observed for the laser cutting and the scoring methods (Figs. 8 and 9).

4 CONCLUSIONS

The results of this work showed that only utilization of sharp and thin tools could not be a reason to produce a sharp pre-crack. Since the tools might be deformed during producing pre-cracks, which caused damage in front of crack tip. This phenomenon, which alters the fracture toughness of samples, was observed in the case of razor blade. The obtained fracture toughness K_{Ic} values showed that in addition to the geometry of crack tip, the K_{Ic} strongly depended on crack tip radius, crack width, and angular or rectangular shape. Moreover, the damage in front of crack, heat affected

zone, and residual stress could be effective on the fracture toughness of samples. Therefore, to decrease the mentioned effects on the fracture toughness of polymeric materials, it would be better to select the method of pre-crack production based on the material type. All of the pre-crack production methods were effective on the fracture toughness of produced notch and producing a pre-crack without any defect was not possible. A sharp crack tip and no sign of damage in front of notch caused lower fracture toughness values. Therefore, scoring method had the lowest value of K_{Ic} , 2.53 MPa.m^{0.5}, and the maximum value of K_{Ic} , 2.77 MPa.m^{0.5}, belonged to metal slitting saw method. The maximum difference resulted from different pre-cracking methods was 0.24 MPa.m^{0.5}. Also, the results indicated that the effects of notching on toughness of RT-PMMA had a low notch sensitivity and the differences between minimum and maximum K_{Ic} values was found about 9%.

NOMENCLATURES

a	Crack length
f(a/w)	Geometrical factor or Non-dimensional stress intensity factor
P_c	Critical load
P_{max}	Maximum load
K_{Ic}	Critical stress intensity factor or fracture toughness
t	Specimen thickness
w	Specimen width
MFI	Melt flow index
\bar{M}_w	Number-average molecular weight
σ_b	Tensile strength at break
σ_y	Yield strength
T_g	Transition temperature
CBN	Cubic boron nitride
HAZ	Heat affected zone
CNC	Computer numerical control
SEM	Scanning electron microscope

References

- Cayard, M. and Bradley, W. (2013). The effect of various precracking techniques on the fracture toughness of plastics. 7th International Conference on Fracture, Houston (USA).
- Choudhury, I., Shirley, S. (2010). Laser cutting of polymeric materials: An experimental investigation. *Optics & Laser technology* 42:503-508.
- Davim, J.P., Barricas, N., Conceicao, M., Oliveira, C. (2008). Some experimental studies on CO₂ laser cutting quality of polymeric materials, *Journal of Materials Processing Technology* 198:99-104.
- El-Sheikhy, R., Al-Shamrani, M. (2015). On the processing and properties of clay/polymer nanocomposites CPNC. *Latin American Journal of Solids and Structures* 12:385-419.
- Gdoutos, E.E. (2005). *Fracture mechanics*, Springer (The Netherlands, Xanthi, Greece 337).
- Ghavidel, A.K., Azdast, T., Shabgard, M.R., Navidfar, A., Shishavan, S.M. (2015). Effect of carbon nanotubes on laser cutting of multi-walled carbon nanotubes/poly methyl methacrylate nanocomposites. *Optics & Laser technology* 67:119-124.

- Hashemi, S., Williams, J. (1984). Size and loading mode effects in fracture toughness testing of polymers, *J. material science* 19:3746-3759.
- Kinloch, A.J. and Young, R.J. (1985). *Fracture behaviour of polymers*, Elsevier Applied Science Publishers (London and New York).
- Kruzic, J., Kuskowski, S., Ritchie, R. (2005). Simple and accurate fracture toughness testing methods for pyrolytic carbon/graphite composites used in heart-valve prostheses, *J. of Biomedical Materials Research Part A* 74:461-464.
- Low, I.M., Mai, Y.W. (1989). Time and temperature effects on the fracture toughness of rigid poly(vinylchloride) pipe materials. *Polymer Engineering & Science* 22:826-831.
- Mandell, J.F., Darwish, A.Y., McGarry, F.J. (1982). Rate and temperature effects on crack blunting mechanisms in pure and modified epoxies, *J. of materials science* 24:1634-1644.
- Marshall, G.P., Culver, L.E., Williams, J.G. (1973). Fracture phenomena in polystyrene. *International Journal of Fracture* 9:295-309.
- Mazidi, M.M., Razavi Aghjeh, M.K., Abbasi, F. (2014). Fractographic analysis of the crack resistance of styrene-acrylonitrile/polybutadiene-g-styrene-acrylonitrile blends as evaluated by the essential work of fracture method. *Applied Polymer Science* 131:40072-40082.
- Needleman, A., Coker, D., Rosakis, A.J. (2005). Fast crack growth along interfaces. *Latin American Journal of Solids and Structures*. 2:3-4.
- Oskui, A.E., Choupani, N., Haddadi, E. (2014). Experimental and numerical investigation of fracture of ABS polymeric material for different sample's thickness using a new loading device. *Polymer Engineering& Science* 54:2086-2096.
- Oskui, A.E., Choupani, N., Shameli, M. (2016). 3D characterization of mixed-mode fracture toughness of materials using a new loading device. *Latin American Journal of Solids and Structures*. 13: 1464-1482.
- Peres, F.M., Schön, C.G., Tarpani, J.R. (2010). Effect of precracking method on K_{Ic} results for medium-density polyethylene tested under cryogenic condition. *Polymer Testing* 29:667-673.
- Peres, F.M., Tarpani, J.R., Schön, C.G. (2014). Essential work of fracture testing method applied to medium density polyethylene. *Procedia Material Science* 3:756-763.
- Salazar, A. and Patel, Y. (2013). Influence of crack sharpness on the fracture toughness of epoxy resins. 13th International Conference on Fracture, Beijing, China.
- Souza, J., Yoshimura, H.N., Peres, F.M., Schon C.G. (2012). Effect of sample pre-cracking method and notch geometry in plane strain fracture toughness tests as applied to a PMMA resin. *Polymer Testing* 31:834-840.
- Wei, Y., DeFranco, S., Dempsey, J. (1990). Crack-fabrication techniques and their effects on the fracture toughness and CTOD for fresh-water columnar ice, *J. glaciology* 37:270-280
- Yan, J., Taskonak, B., Platt, J.A., Mecholsky Jr, J.J. (2008). Evaluation of fracture toughness of human dentin using elastic-plastic fracture mechanics, *J. biomechanics* 41:1253-1259.